The International Journal of Advanced Manufacturing Technology (2019) 101:603–614
https://doi.org/10.1007/s00170-018-2942-5

ORIGINAL ARTICLE

An optimized fuzzy-genetic algorithm for metal foam manufacturing process control

Gennaro Salvatore Ponticelli[1] · Stefano Guarino[1] · Vincenzo Tagliaferri[2] · Oliviero Giannini[1]

Received: 23 February 2018 / Accepted: 26 October 2018 / Published online: 6 November 2018

Abstract

The present investigation deals with the proposal of a combined fuzzy-genetic algorithm (F-GA) model able to describe the inherent uncertainties related to the manufacture of open-cell aluminum foams by using the dissolution and sintering process (DSP). The use of the F-GA method allows to take into account, within the same model, both the uncertainty related to the model and the statistical manufacturing process variability. The developed model is aimed at controlling the capability of this material at absorbing energy in compressive deformation, for a different set of process parameters. In particular, the use of genetic algorithms allows the optimization of the support of the fuzzy numbers defined in the model in order to take into account most of the experimental data in combination with the smallest uncertainty. Then, the input uncertainty, related to both the process variability and the chosen model, is propagated to the output variables by the Transformation Method. The fuzzy results are then compared with the measured data and the membership level of the dataset to the uncertain model is evaluated. The process maps generated allow to select the operational parameters in order to obtain a desired process output, in combination with the lowest uncertainty level, providing, as additional information, how much the uncertainty of the model and the process varies by changing those operational parameters.

Keywords Fuzzy logic · Genetic algorithm · Transformation method · Metal foams · DSP

1 Introduction

In the last decades, metal foams have become increasingly attractive for their interesting physical, mechanical, thermal, electrical, and acoustic properties. Foam combines part of the characteristics of a bulk metal with the structural advantages of a foam [1, 2], offering potential for lightweight structures [3], for energy absorption [4–7], and for thermal management [8–12]. Both the attention and the progress in crashworthiness of vehicles have experienced a significant improvement, focusing the design on the passenger safety. The current philosophy adopted in the automobile industry is to structurally harden the passenger compartment against collapse and intrusion. Then, the features of metallic foams make them suitable to applications requiring high stiffness-to-weight ratio and efficient energy absorption. The challenge is to employ these innovative materials in a controlled manner [13]. The improvement of many manufacturing techniques has allowed the development of different foaming processes, making it possible to easily control the shape and distribution of the space holders as well as the morphology of the porosity in the foams, promoting an improved repeatability, which allows designing the material properties by simply choosing the characteristics and the amount of the space holder [14].

The main interest of manufacturers is the optimization of the production and the subsequent quality of components. However, both aspects are governed by a complex interaction between the process parameters and the properties of the processed materials. In particular, the parameters are usually adjusted and tuned one by one to obtain the desired quality [5, 6, 15–18]; however, this approach consumes time and effort. At the same time, foam quality cannot be easily predicted. To date, many studies have been aimed at analyzing the foam processing based on Analytical Modeling [19–21] and Numerical Modeling [8, 19, 22]. In the first case, modeling

✉ Gennaro Salvatore Ponticelli
gennaro.ponticelli@unicusano.it

[1] Department of Engineering, University 'Niccolò Cusano', Via Don Carlo Gnocchi3, 00166 Rome, Italy

[2] Department of Enterprise Engineering, University 'Tor Vergata', Via del Politecnico, 1, 00133 Rome, Italy

based on an analytical solution is usually centered on some assumptions oversimplifying the problem and overestimating or underestimating the solution [19]. On the other hand, the lack of reliable, comprehensive, and yet computationally fast physical models of such a multivariable system still makes numerical modeling of technological processes a difficult, if not impossible task.

In this light, engineering problems which involve complexity and non-linearity, such is the foam manufacturing process, have benefited from artificial intelligence (AI)-based methods [23–26]. These methods use mathematical tools and treat the model as a black-box dealing only with input-output relations, thus overcoming all the model complexity. Moreover, AI models are able to handle vague information without requiring knowledge of internal system parameters and providing a compact solution for multivariable problems [27, 28].

Several process routes have been developed to make metal foams [3]. However, some drawbacks as low process repeatability, its unsuitability in manufacturing of complex shapes, and high associated running and plant costs constitute an additional limit to the ultimate development of foam production technologies [2, 14]. Most of this problems may be solved by using a novel process, named Dissolution and Sintering Process (DSP), which consists of four main steps [29]: (i) mixing the starting metal powder with the space-holder particles (SHP); (ii) compacting the mixture in order to obtain a green compact; (iii) dissolution of the SHP with an appropriate solvent in order to obtain a cellular structure; (iv) sintering of the latter structure to produce metallurgical bond among the metallic powders. In this way, the shape and distribution of the space holders as well as the morphology of the porosity in the foams can be easily controlled. In general, DSP is a flexible process by which many different pore sizes and densities can be produced. However, the achievement of the desired characteristic for the considered application could be time and effort consuming, since the manufacturing process parameters should be accordingly tuned. For this reason, empirical-, numerical-, and artificial intelligence-based methods can be applied in order to find the optimal operational parameters. However, since this kind of process suffers from a strong process variability and hence a low repeatability, traditional statistical approaches may fail at identifying which factors are the most influential. On the other hand, models that include all the factors and the interactions, thus very complicated, may be unsuitable for modeling and prediction. Moreover, even complicated models still will represent only the median process leaving the user with little information about the dispersion around the mean. For this reason, more uncertain models based on expert systems such the fuzzy logic with genetic algorithms optimization can be considered a valuable alternative for modeling the experimental data and for simulation purposes.

Several papers have been recently published in the scientific literature regarding the application of the fuzzy theory to the optimization of the manufacturing processes [30–33], but none of them concerns the manufacturing process of the metal foams. In this light, the present study is aimed at proposing a combined fuzzy-genetic algorithm (F-GA) approach able to describe the inherent uncertainties related to a DSP foam manufacturing process, with the aim of predicting the resulting absorbing energy properties and the compressive deformation behavior, for different set of process parameters, i.e., weight percentage of carbamide particles, mesh size of carbamide particles, and compression speed, which are suggested to be the main control factors by the ANOVA test carried out on existing experimental data. The use of the genetic algorithm allows the optimization of the support of the fuzzy model in order to take into account most of the experimental data in combination with the smallest uncertainty level. Then, the input uncertainty, related to both the process variability and the chosen model, is propagated to the output variables by the Transformation Method. The fuzzy results are compared with the measured data and the membership level of the dataset to the uncertain model was evaluated. The process map obtained by the application of the fuzzy model is used to select operational parameters in order to obtain a desired process output, providing as additional information how much the uncertainty of the model and the process varies by changing operational parameters. The large variability of the process is highlighted by the proposed model through a large band of uncertainty that occurs in the process map generated. The F-GA model has also been used to assess the optimal parameters in order to satisfy the requirement of the highest energy absorption and the lowest deformation in combination with the lowest level of uncertainty.

2 Process engineering control: F-GA modeling

Generally speaking, the implementation of a direct model able to accurately describe the effect of control parameters on the quality of technological process is a challenging task due to the inherent variability of the process, which derives from the complex nature of the process, and the approximation introduced in the model, which is typically due to the lack of knowledge on the physics occurring into the process itself.

The source of uncertainty related to a manufacturing process is usually random and can be easily modeled with stochastic methods provided that enough experimental data are available. On the other hand, statistics is not useful in modeling the systematic error introduced by model approximations. In the latter case, fuzzy arithmetic can be considered a viable alternative [27, 34, 35]. In other words, the advantage of using fuzzy modeling is related to the possibility to model at the same time both the systematic and the random errors [30].

2.1 Fuzzy model optimization

The fuzzy model, proposed in a previous work [30], implements the Transformation Method [36] that performs a mapping of points in the input parameter hyperspace onto points in the output space, reducing the fuzzy arithmetic to a set of operations for the intervals at each α-cut by avoiding standard interval arithmetic, as defined by Moore [37], and with the purpose of finally obtaining a quantification of the uncertainties in the output variables. Each input interval is sampled independently from the others. Therefore, at each α-level, the hyper-interval in the input space is defined by the Cartesian product between each vector representing each sampled interval. Moreover, the fuzzy model can also be numerically inverted to evaluate the samples that are described by the model for a given membership level. In other words, it is possible to first assign the desired output value and then calculate those scenarios that satisfy that initial condition.

In [30], the support of each fuzzy parameter was chosen in order to take into account most of the experimental data, according to the confidence level of 95%. This, however, because of the non-stochastic nature of the model uncertainty, resulted in the loss of several data points (about 20%). Moreover, the extent of the uncertainty region provided by the fuzzy model, which is directly related to the confidence level adopted, increases as the number of the data points considered increases, e.g., by increasing the confidence interval to 99% there is a corresponding reduction to about 10% of the data points excluded but with a far less precise estimation of the model output. In this light, it is here proposed a genetic algorithm in order to optimize the extent of the uncertainty region according to a fixed number of experimental data to take into account.

2.2 Genetic algorithm

Genetic algorithms procedure generally consists of four steps [38], i.e., initialization, crossover, selection, and mutation. Furthermore, two other important concepts are the genetic coding of the parameters and the formulation of the fitness function.

A chromosome represents an individual solution in the population. Encoding of chromosomes is one of the first choices to make when using genetic algorithms. The principal types of encoding are binary, permutation, value, and tree. In this study, the binary encoding is used, in which every chromosome is a string of bits. In particular, the values of the statistic confidence intervals are encoded in the genes of the chromosome.

The initial population of models is generated randomly, and it evolves into the next generation by genetic operators, crossover (i), mutation (ii), and selection (iii).

(i) The crossover is performed between two selected individuals, called parents, by exchanging parts of their strings, which start from a randomly chosen crossover point. Among the crossover types, in this study, the single-point crossover is considered and the site for the crossover operation is selected randomly on every chromosome.

(ii) The mutation is used to avoid local convergence of the algorithm [39], by introducing random variation in the genome of some individuals. While increasing the number of generations, chromosomes are similar to each other even if a high crossover rate is determined. This situation blocks diversity and prevents the occurrence of more powerful generations. For this purpose, the mutation operator is used to increase the diversity of chromosomes in population by altering one or more genes. In particular, the mutation operator only starts after some new generations with a fixed probability of occurrence, which in this case is set at 50%. A single-point mutation is considered and the site for the mutation operation is selected randomly on every chromosome.

(iii) Some of the chromosomes in the population can be transferred to the next generation, while some of them are eliminated. The selection operator decides which chromosome will be transferred to the next generation, by using selection probabilities of each chromosome. Several methods such as roulette-wheel, ranking, tournament, and sharing, have been introduced for selecting genomes. In this case, the ranking method was adopted. In particular, the selection of the individuals takes place through sorting accordingly to their fitness values obtained using an objective function. Rank selection first ranks the population and then every chromosome receives fitness from this ranking. The worst will have fitness 1, second worst 2, etc., and the best will have fitness N (number of chromosomes in population). Then, the first 50% of the best individuals are chosen to mate. In particular, according to the target of this research study, the fitness function returns the lowest extent of the uncertainty region in combination with the highest number of the experimental data to consider. Specifically, this was achieved by defining an appropriate weight between the two variables. The details are given in the following section.

Table 1 Materials characteristics

Materials	Grade (%)	Size (μm)	Factor shape
Aluminum powder	99.98	10	0.8
Carbamide particles	98	0.841–1.680	0.95

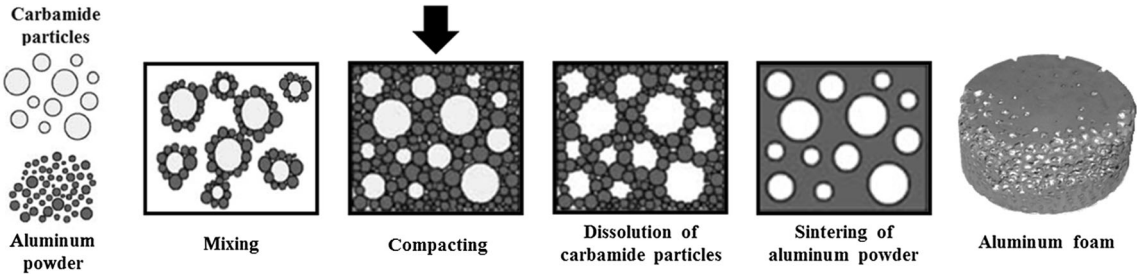

Fig. 1 DSP process highlights

3 Case study: open-cell aluminum foam DSP manufacturing process

In the considered study [14], green samples were made from aluminum powder (supplied by Pometon Srl., Italy) and carbamide ($(NH_2)_2CO$) particles (supplied by Aldrich Ltd., USA), whose characteristics are reported in Table 1. The resulting dense paste was moved into a round-bottomed flask and mixed and dried using a rotary evaporator (Heidolph Rotavapor model 4000) at 40 °C bath temperature and reduced pressure (vacuum pump Chemat Technology model KW-AVP). The resulting mixtures were compacted into a built ad hoc stainless steel cylindrical mold using a static test machine (MTS model Alliance RT/50). Dissolution of carbamide particles was operated in a hot water bath (Heidolph Rotavapor model 4000) at about 70 °C and for 1 h, under strictly monitored conditions. The dissolution rate was verified by weighting the sample before and after the dissolution and drying phase. In order to prevent oxidation of the compacted but still not sintered aluminum powders, drying of the precursors was performed in an evacuated drying chamber (Binder model VD 23) overnight at 40 °C. Sintering was subsequently performed under low vacuum conditions (10^{-3} Pa) in a convective furnace (Proba model VF1900) equipped with a diffusion pump. Sintering temperature and time was fixed at 540 °C and 1 h, respectively. In Fig. 1 are represented the main steps of the DSP foam manufacturing process here described.

Figure 2 shows FE-SEM micrographics of the structure of the precursor after the compaction (Fig. 2a) and the precursor after the dissolution of the carbamide (Fig. 2b). In particular, as shown in Fig. 2a, carbamide particles, (darker zones) are encased in the aluminum matrix (clearer zones), preserving almost their spherical shape, while Fig. 2b emphasizes the good distribution of the porosity inside the precursor.

The overall mechanical properties of the samples were characterized by means of compression tests performed with the same static test machine used during the aforementioned compacting step. Load speed was set at 1 mm/min. Figure 3 reports the typical output of the compression tests performed. As shown in the latter, the compressive deformation behavior ΔL is the sum of the deformation during the elastoplastic and extended plateau zone, while the mechanical energy absorption E is represented by the hatched area.

Since a large number of parameters are involved in the foam manufacturing process, the experimental tests were scheduled according to the developed full factorial plan based on Design of Experiment (DoE), which is reported in Table 2, for a total of 18 process scenarios (3 terms of $C_{\%}$ · 3 terms of C_{MS} · 2 terms of S). Tests were repeated, at least, five times for a total number of 90 experiments. It is worth to note that in this study, among the pressures examined in [14], only the value of 300 MPa was maintained, because of the change in shape of the carbamide particles when compacted under higher pressure values (i.e., 400 and 500 MPa), which does not ensure the realization of homogenous spherical-like cells in the foams (as highlighted in Fig. 2a by the dashed red circle).

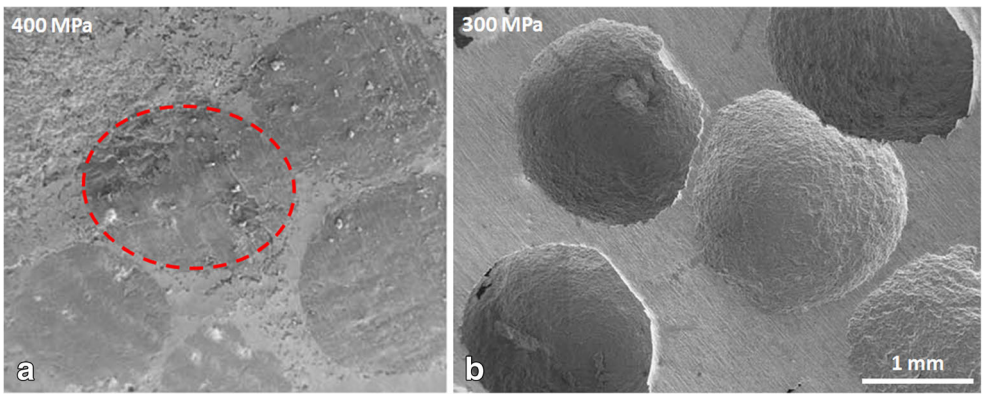

Fig. 2 FE-SEM images of an open-cell aluminum foam: (**a**) compacted aluminum powders with carbamide particles; (**b**) precursor after the dissolution process. The dashed red circle highlights the ovalization of the carbamide particles occurring increasing the compaction pressure

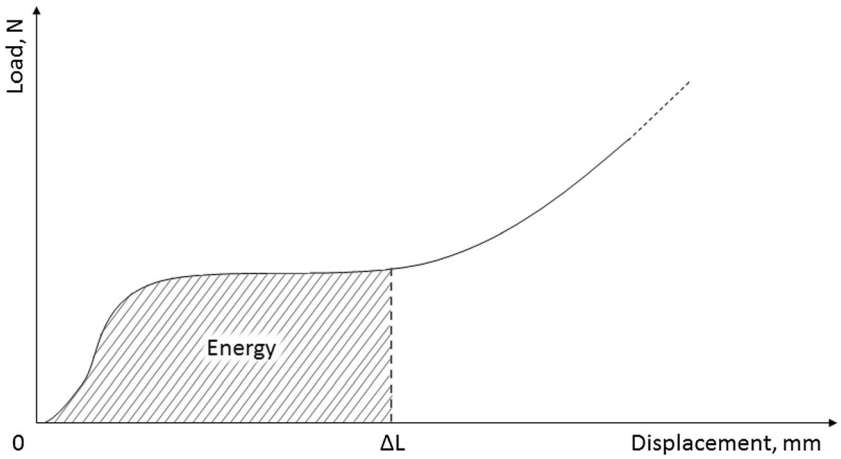

Fig. 3 Typical output of the compression tests performed

3.1 ANOVA test

The statistical significance of the control factors ($C_{\%}$, C_{MS}, S) for the ΔL and E response variables are evaluated by using the ANOVA test. The results consist of a table containing the degrees of freedom (DoF), the adjusted sum of squares (Adj.SS), the adjusted mean squares (Adj.MS), the F value, the p value, and the contribution percentage (Π) of each parameter or parameter combination. In general, the term Adj.SS provides the variation of each parameter with respect to the response variables. This information is quantified by the Π term, which is the ratio between the Adj.SS term of the analyzed parameter and the total one. The F value is used to determine whether a term is associated with the response, comparing the result with the corresponding tabulated value (3.87 for 1-DoF and 3.03 for 2-DoF): the greater the F value the greater the influence on the response variable. In this case, the F value is defined as the ratio between the Adj.MS value of the response variable investigated and the Adj.MS of the error. Finally, the p value is used to determine the significance of the factors (the analysis was carried out at a 95% confidence level; thus, a process parameter or their combination is considered significant if the p value is lower than 0.05). Tables 3 and 4 show the ANOVA results for the energy absorption and the deformation, respectively, in which the F value, the p value, and the Π term of each significant effect are highlighted by the italicized text (i.e., p value < 0.05, $\Pi > 5\%$, F value > 3.984 for 1-DoF, F value > 3.134 for 2-DoF, and F value > 2.594 for 4-DoF).

As reported in Tables 3 and 4, the weight percentage of carbamide particles ($C_{\%}$) was found to be of major influence for both the energy and the compressive deformation. In particular, increasing $C_{\%}$ means decreasing the amount of energy the foam can absorb during its compression. This result can be attributed to the loss of rigidity of the structure due to the massive presence of porosities [14, 40]. On the other hand, the low value of contribution percentage of mesh size of carbamide particles (C_{MS}) could suggest the rather low capability of such experimental factor to induce systematic variation in the energy absorption and deformation. Even compaction speed was found to be characterized by a very low Π term, especially for the compressive deformation. In any case, the understanding of which factor and/or interaction is significant or not cannot be drawn by a simple examination of p values, F values, and related contribution percentages. In fact, experimental data are nearly homoscedastic. This determines Fischer's factors largely bigger than the corresponding values tabulated and do not allow to deduce conclusions about the meaningfulness of each investigated factor and interaction [41]. However, a certain interest can be found in the analysis of the interaction between the two factors ($C_{\%}$ and S), which were found to induce the most relevant systematic variations in particular for the energy output, while the major contribution on the deformation output is given by the triple interaction $C_{\%}{\cdot}C_{MS}{\cdot}S$. Accordingly, all the factors and interactions should be considered in the model and, for this reason, in the present study, a sophisticated model based on fuzzy logic with further support of genetic algorithms, with the aim of minimizing the conservativeness of the model, have been selected for modeling the experimental data and for simulation purposes.

Table 2 Full factorial plan: 3 terms of $C_{\%}$ 3 terms of C_{MS} 2 terms of S 5 replications = 90 tests

Parameters	Values			Units
Weight percentage of carbamide particles ($C_{\%}$)	40	50	60	wt%
Mesh size of carbamide particles (C_{MS})	12 (0.841)	16 (1.190)	20 (1.680)	– (μm)
Compaction speed (S)	1		10	mm/min

Table 3 ANOVA results for the energy absorption E

Source	DoF	Adj.SS	Adj.MS	F value	p value	Π (%)
$C_{\%}$ (wt%)	2	2.82073	1.41036	*4045.90*	**0**	*50.02*
C_{MS}	2	0.45969	0.22985	*659.35*	**0**	*8.15*
S (mm/min)	1	0.42745	0.42745	*1226.22*	**0**	*7.58*
$C_{\%} \cdot C_{MS}$	4	0.35117	0.08779	*251.85*	**0**	*6.22*
$C_{\%} \cdot S$	2	0.44267	0.22134	*634.94*	**0**	*7.85*
$C_{MS} \cdot S$	2	0.92855	0.46427	*1331.86*	**0**	*16.47*
$C_{\%} \cdot C_{MS} \cdot S$	4	0.18399	0.04600	131.95	0	3.26
Error	72	0.02510	0.00035			0.45
Total	89	5.63934				

3.2 Empirical modeling

Based on the results of the ANOVA tests, an empirical model of the foam manufacturing process has been proposed for both the output variables E and ΔL. In this case, the empirical models only consider the experimental parameters and their interactions whose calculated p values are greater than 0.05; Fisher's factors are bigger than corresponding Fisher's factors tabulated and characterized by a percentage of contribution of, at least, 5%. In particular, regarding the energy absorption, the experimental factors $C_{\%}$, C_{MS}, S, and the interactions $C_{\%} \cdot C_{MS}$, $C_{\%} \cdot S$ as well as $C_{MS} \cdot S$ are considered, while for the deformation, the factors $C_{\%}$, C_{MS} and the interactions $C_{\%} \cdot C_{MS}$, $C_{\%} \cdot S$, $C_{\%} \cdot C_{MS} \cdot S$ were taken into account.

The numerical formulations of the empirical models can be drawn as follows:

$$E = \mathcal{F}(C_{\%}, C_{MS}, S) = a_E \cdot C_{\%} + b_E \cdot C_{MS} + c_E \cdot S + d_E \cdot C_{\%} \cdot C_{MS} + e_E \cdot C_{\%} \cdot S + f_E \cdot C_{MS} \cdot S + g_E \quad (1)$$

Table 4 ANOVA results for the deformation ΔL

Source	DoF	Adj.SS	Adj.MS	F value	p value	Π (%)
$C_{\%}$ (wt%)	2	0.75359	0.376793	*919.91*	**0**	*14.36*
C_{MS}	2	0.64436	0.322181	*786.58*	**0**	*12.28*
S (mm/min)	1	0.11053	0.110534	269.86	0	2.11
$C_{\%} \cdot C_{MS}$	4	2.03194	0.507985	*1240.20*	**0**	*38.72*
$C_{\%} \cdot S$	2	0.39850	0.199248	*486.45*	**0**	*7.59*
$C_{MS} \cdot S$	2	0.16417	0.082086	200.41	0	3.13
$C_{\%} \cdot C_{MS} \cdot S$	4	1.11515	0.278788	*680.64*	**0**	*21.25*
Error	72	0.02949	0.000410			0.56
Total	89	5.24774				

Table 5 Calibration coefficients values and their 95% confidence intervals for the energy absorption E

Calibration coefficients	Values	95% confidence intervals
a_E	0.0073	− 0.0089; 0.0235
b_E	0.1088	0.0590; 0.1586
c_E	0.2062	0.1611; 0.2514
d_E	− 0.0012	− 0.0021; − 0.0002
e_E	− 0.0016	− 0.0023; − 0.0009
f_E	− 0.0069	− 0.0087; − 0.0052
g_E	− 0.7297	− 1.5648; 0.1054

$$\Delta L = \mathcal{G}(C_{\%}, C_{MS}, S) = a_{\Delta L} \cdot C_{\%} + b_{\Delta L} \cdot C_{MS} + c_{\Delta L} \cdot C_{\%} \cdot C_{MS} + d_{\Delta L} \cdot C_{\%} \cdot S + e_{\Delta L} \cdot C_{\%} \cdot C_{MS} \cdot S + f_{\Delta L} \quad (2)$$

where the constant g_E and the empirical coefficients a_E, b_E, c_E, d_E, e_E, f_E, related to the energy absorption, and the constant $f_{\Delta L}$ and the empirical coefficients $a_{\Delta L}$, $b_{\Delta L}$, $c_{\Delta L}$, $d_{\Delta L}$, $e_{\Delta L}$, related to the deformation, are used as calibration coefficients in the fuzzy model definition. They were determined by nonlinear multiple regression analysis based on the whole experimental dataset and are reported in Tables 5 and 6, in which are also presented the corresponding 95% confidence intervals.

3.3 Fuzzy-genetic algorithm model

The aim is to produce a fuzzy input-output relation, based on experimental observations, that links the control factors highlighted by the ANOVA test (weight percentage of carbamide, mesh size of carbamide, and compaction speed) to the achieved energy absorption E and deformation ΔL. The model can be used to evaluate how much a given experimental sample, characterized by a certain value of $C_{\%}$, C_{MS}, S, and the corresponding E and ΔL, belong to the fuzzy set defined by Eqs. 3 and 4: the idea is to start from the regression expressions used to empirically model the DSP process (see Eqs. 1 and 2), with a different definition of the coefficients, which in this case become fuzzy numbers, highlighted in the Eqs. 3 and

Table 6 Calibration coefficients values and their 95% confidence intervals for the deformation ΔL

Calibration coefficients	Values	95% confidence intervals
$a_{\Delta L}$	− 0.0045	− 0.0331; 0.0241
$b_{\Delta L}$	− 0.0238	− 0.1109; 0.0632
$c_{\Delta L}$	0.0008	− 0.0010; 0.0025
$d_{\Delta L}$	− 0.0004	− 0.0014; 0.0006
$e_{\Delta L}$	0.0000	− 0.0000; 0.0001
$f_{\Delta L}$	0.4462	− 0.9751; 1.8675

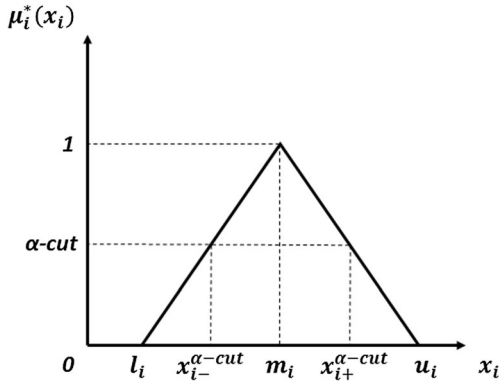

Fig. 4 Triangular Fuzzy number

4 by the asterisk. It is important to notice that the values of the process parameters are measured and deterministic thus remain a regular number, while the uncertainty is modeled within the fuzzy coefficients.

$$E^* = F^*(C_\%, C_{MS}, CS) = a_E{}^*\cdot C_\% + b_E{}^*\cdot C_{MS} + c_E{}^*\cdot S + d_E{}^*\cdot C_\%\cdot C_{MS} + e_E{}^*\cdot C_\%\cdot S + f_E{}^*\cdot C_{MS}\cdot S + g_E{}^* \quad (3)$$

$$\Delta L^* = G^*(C_\%, C_{MS}, CS) = a_{\Delta L}{}^*\cdot C_\% + b_{\Delta L}{}^*\cdot C_{MS} + c_{\Delta L}{}^*\cdot C_\%\cdot C_{MS} + d_{\Delta L}{}^*\cdot C_\%\cdot S + e_{\Delta L}{}^*\cdot C_\%\cdot C_{MS}\cdot S + f_{\Delta L}{}^* \quad (4)$$

In both cases, it is possible to state that, the nominal models (Eqs. 1 and 2) do not represent any experimental data (i.e., there is no experimental evaluation that can fall over the model surface). As the level of uncertainty is increased, measured by a decrease in the membership function, the model accommodates a larger number of samples with lower membership level. In other words, the fuzzy model is able to describe, as the membership function decreases, an increasing number of experimental data and, thanks to the genetic algorithm, with the highest degree of belonging to the fuzzy set defined by the model itself.

In Eqs. 3 and 4, all the fuzzy regression coefficients are independent triangular fuzzy numbers (Fig. 4) whose membership functions $\mu_i^*(x_i)$ are described by Eq. 5.

$$\mu_i^*(x_i) = \begin{cases} 0, & x_i < l_i, x_i > m_i \\ \frac{x_i - l_i}{m_i - l_i} & l_i \le x_i \le m_i \\ \frac{u_i - x_i}{u_i - m_i} & m_i \le x_i \le u_i \end{cases} \quad (5)$$

A triangular fuzzy number is characterized by three values: a lower bound (l_i), an upper bound (u_i), and a modal (or peak) value (m_i). The modal value has a membership function $\mu_i^*(x_i) = 1$, the highest possible set membership for the uncertain parameters. When the value of the parameter reaches the lower bound (or upper bound) the degree of belief that this value truly represents, the chosen parameter is reduced to zero. Finally, the interval (l_i, u_i) represents the support of the membership function. Each of the fuzzy regression coefficients has the modal value coinciding with the results provided by the linear regression, while the support is defined by the genetic algorithm, according to the fitness function (Eq. 6):

$$fit\ value = w\cdot\frac{n}{N} + (1-w)\frac{H_V}{H_C} \quad (6)$$

where w represents a weighting term, n refers to the number of data not taken into account, and H_V is the hypervolume covered by the F-GA model and related to the uncertainty dispersion of the considered data. As reported in Eq. 6, each term is opportunely normalized in order to have two comparable quantities. In particular, the first term is normalized by using the total number of the available data N, while the second term is normalized by using the hypercube including all the data. The use of such a fitness function is aimed at controlling the highest number of considered data in combination with the lowest hypervolume at $\mu_i^*(x_i) = 0$.

All the fuzzy parameters are described by 8 α-cut and the interval at each α-level is discretized with $N_s = 2$ points. For each α-cut, the transformation method requires, in a combinatorial scheme, the evaluation of N_s to the power of the number of fuzzy parameters $N_E = 7$ models for the absorption energy

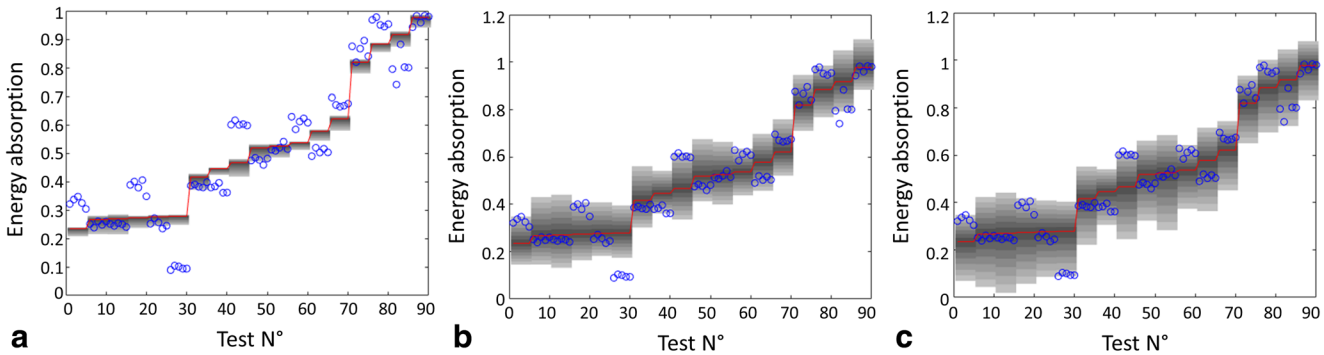

Fig. 5 Genetic algorithm optimization: (**a**) w= 0.2; (**b**) w= 0.4; (c) w= 0.6

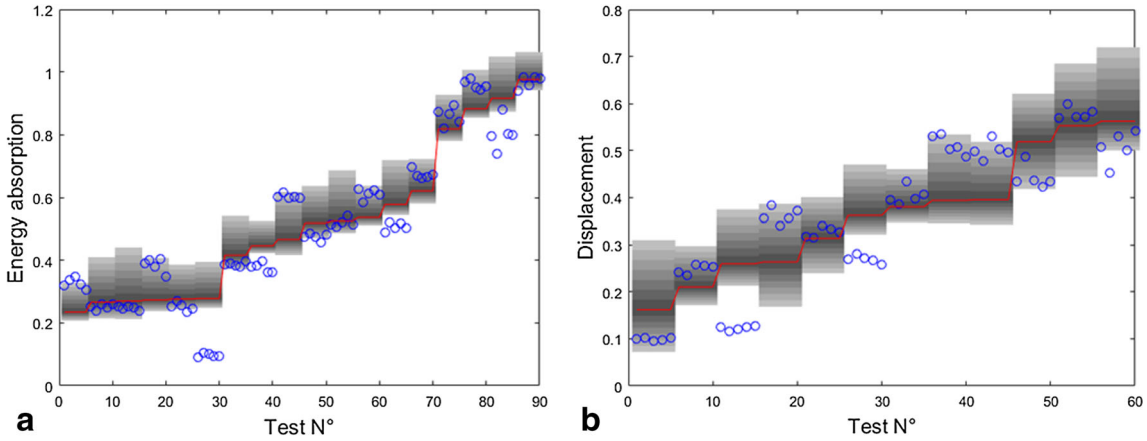

Fig. 6 Results of the Transformation Method (gray shaded area), experimental results (blue circles), nominal model results (red line) for (**a**) energy absorption E and (**b**) deformation ΔL

and $N_{\Delta L} = 6$ models for the deformation, leading to 128 and 64 evaluations, respectively.

The Transformation method requires that, for each α-cut, all these models are evaluated obtaining for each of them the hypersurface of the output quantity (e.g., the energy absorbed E) as a function of the process parameters (i.e., $C_{\%}$, C_{MS}, S). The fuzzy result for the given α-cut is then obtained by computing the envelope of these hypersurfaces.

The results of the genetic algorithm optimization are reported in Figure 5. The experimental data, ordered for increasing value of energy absorption obtained by the nominal model, are represented as blue circle and the F-GA model results are represented by the shaded area, where lighter zones refer to lower membership level.

As shown in the latter figure, increasing the weight, w, both the number of data covered by the model and the width of the fuzzy bands increase. However, Fig. 5a shows that a too low w value involves very few data, while a too high w value (see Fig. 5c) results in a too large dispersion of the fuzzy uncertainty bands, even if the model is able to take into account all the experimental data. Among all the weight values investigated, the most suitable was 0.27. The results obtained applying this weight are presented in Fig. 6, in which the samples are ordered for increasing values of E (Fig. 6a) and ΔL (Fig. 6b) provided by the nominal models (red line).

From the inspection of the fuzzy results reported in Fig. 6, the uncertainty level related to the fuzzy models appears to be not constant with respect to the parameter combination used during the experimental test for both the energy absorption and the deformation. It is worth to note that the extent of the input uncertainty in the model, due to the choice of a specific confidence interval, is not only related to the accuracy of the regression model adopted but also to the variability of the process. So, the transformation method, which in this case was used to propagate the uncertainty to the outputs, also provides information about the uncertainty at the input level due to the regression model adopted. This effect can be therefore considered the reason for a non-constant level of uncertainty.

In general, this kind of process map can be used to select operational parameters in order to obtain a desired process output. They provide, as additional information, how much

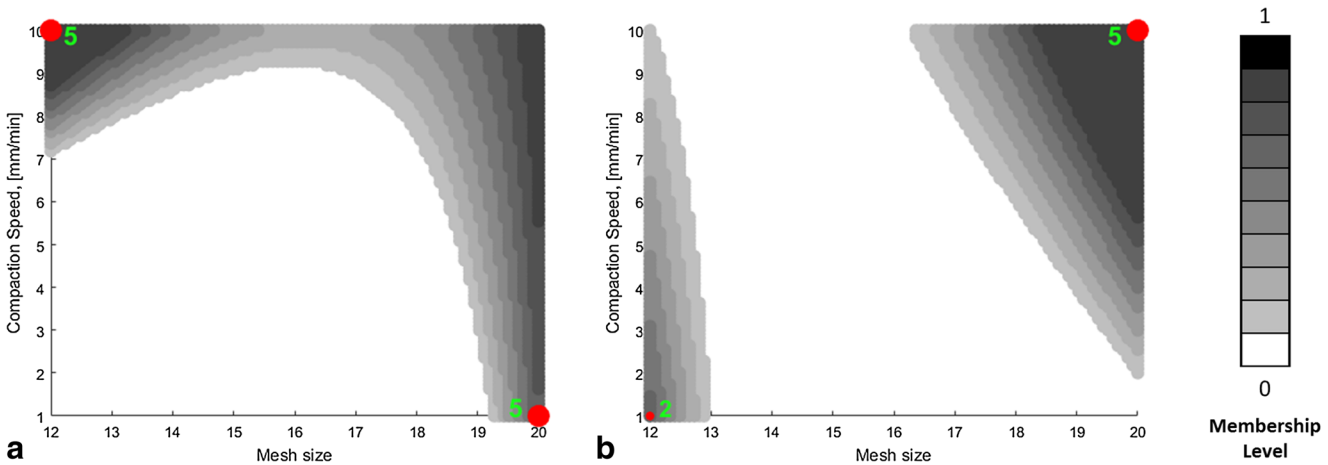

Fig. 7 Fuzzy maps with experimental occurrences (red dots and green numbers) obtained for $C_{\%} = 40\%$: (**a**) $E > 90\%$ and (**b**) $\Delta L < 50\%$

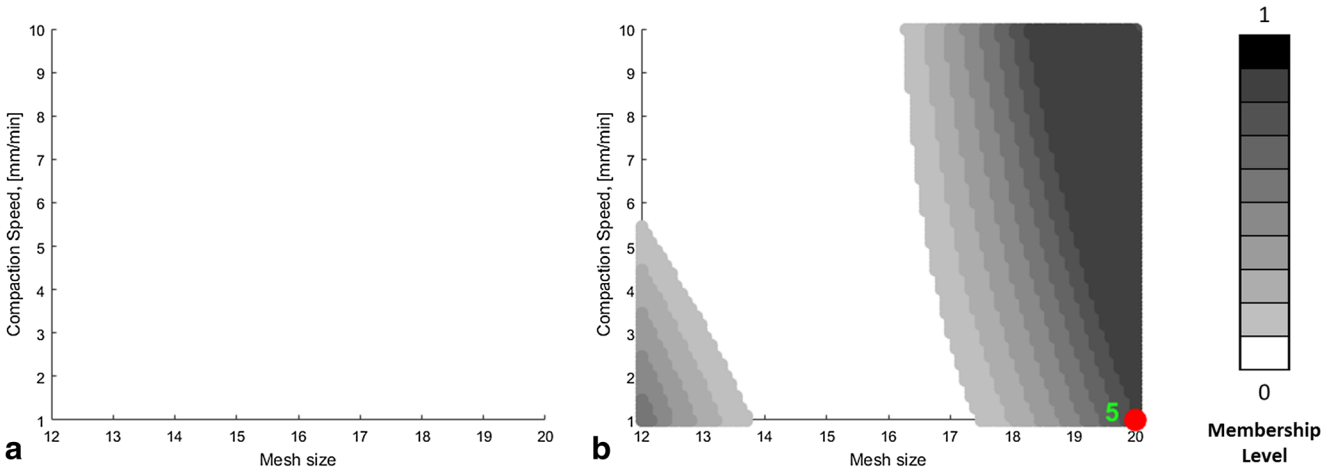

Fig. 8 Fuzzy maps with experimental occurrences (red dots and green numbers) obtained for $C_{\%} = 50\%$: (**a**) $E > 90\%$ and (**b**) $\Delta L < 50\%$

the uncertainty of the model and the process varies by changing operational parameters. It is important to notice here that the large variability of the process is highlighted by the combined fuzzy-genetic algorithm model through a large band of uncertainty, represented in the latter figure by gray shaded areas. Moreover, it is worth to note that this information is not available by considering just the nominal regression model, nor directly obtained from the values of the confidence interval. Finally, for this case study, the F-GA results warn the analyst on the high level of uncertainty, which is inherently present in the investigated foam manufacturing process.

The proposed model can also be inverted so that it is possible to obtain the most suitable operational parameters leading to a desired output. For the case study, the fuzzy model has been used to assess the optimal parameters in order to satisfy the highest energy absorption in combination with the lowest deformation requirement. This combination is useful for crashworthiness purposes. In fact, in crash situations, in order to ensure the safety of occupants inside a vehicle, the restraint structures should assure the highest absorption of the kinetic energy, minimizing crash loads transferred to the vehicle occupants, and at the same time, these systems should control the deformation areas in order to maintain the adequate space in a passenger cell and avoid intrusion of the surrounding structure.

The results can be represented in two-dimensional graphs by varying the input parameters one by one while fixing the others. In this way, different maps for each parameter combinations can be drawn. Figure 7 shows the results obtained by applying the inverse fuzzy approach fixing the weight percentage of the carbamide to 40%, while varying the other two terms, i.e., the mesh size of the carbamide and the compaction speed. In particular, the fuzzy maps are obtained in order to satisfy the highest energy absorption requirement (Fig. 7a), which in this case was set over 90% of the highest value of the absorbed energy obtained in the experimental tests, while maintaining small deformation (Fig. 7b), set below 50% of the maximum level measured. Figure 8 shows the results obtained

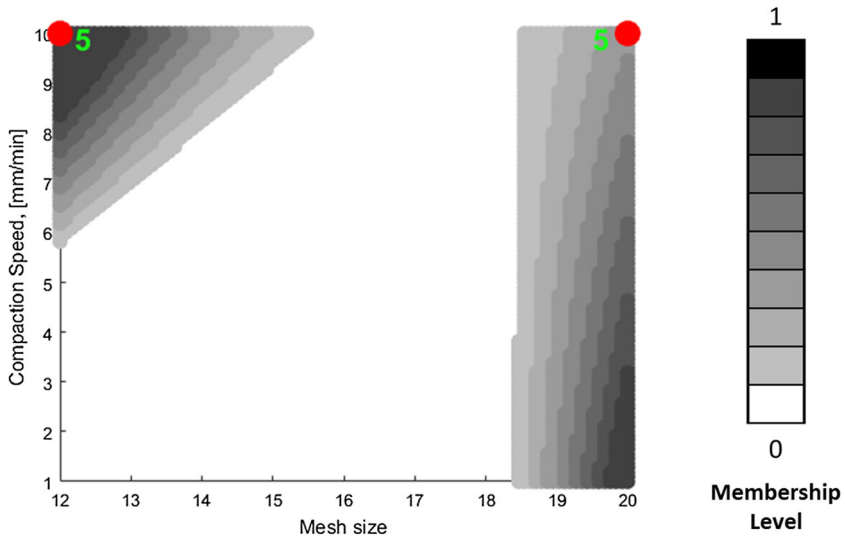

Fig. 9 Fuzzy maps with experimental occurrences (red dots and green numbers) obtained for $C_{\%} = 50\%$ and $E = 55\%$

for $C_{\%} = 50\%$. For both Figs. 7 and 8, the membership level of the fuzzy model is represented as a gray shaded area, while the experimental data and their occurrences as red dots (the dimension of each dot is proportional to the number of occurrences reported as green numbers respectively).

The maps highlight that for $C_{\%} = 40\%$, in terms of energy absorption (Fig. 7a), it is possible to range along the whole axis of the compaction speed at the largest size of carbamide particles ($C_{MS} = 20$) and along the whole axis of the mesh size at the highest compaction speed ($S = 10$ mm/min). However, the best result is given by the combination of the lowest value of S with the largest size of C_{MS}, because it is characterized by the smallest uncertainty dispersion width. On the other hand, in terms of deformation (Figure 7b), the requirement can be satisfied for any value of the compaction speed in combination with the smallest and largest C_{MS}. But, in order to have the lowest uncertainty dispersion, the best combination is given by $S =$ 1 mm/min and $C_{MS} = 12$. However, since the goal is to find the best solution that satisfies both requirements at the same time, the combination of the highest compaction speed and the largest size of carbamide particles can be considered the optimum, even if the fuzzy maps suggest that in this scenario, the uncertainty is quite dispersed compared to the average nominal value. It is worth to note that from the experimental point of view, this solution was measured but with an energy absorption value slightly lower, i.e., 88% instead of 90%.

By increasing the percentage of carbamide particles to $C_{\%} = 50\%$ (Fig. 8), for the energy absorption there is not any solution that can satisfy the requirement of $E > 90\%$. This is highlighted in Fig. 8a by the fact that the fuzzy map obtained is empty, while for the deformation, all the range of S can be used. This is true, in particular, at the highest value of C_{MS}. It is worth to note that for $C_{\%} = 50\%$, it is possible to find a valuable solution only for an absorbing energy level of 55% of the highest value measured in the experimental tests (see Fig. 9). In the latter case, the combination with a low deformation (Fig. 8b) can be satisfied, even in this case, by adopting $S = 10$ mm/min and $C_{MS} = 20$.

Each of these maps provides a relation between S, C_{MS}, and E or ΔL, so each of them can be used to select the optimal level considering both the desired output and uncertainty. In this case study, for both E and ΔL, it is therefore convenient to use large carbamide particles ($C_{MS} = 20$) which lead to large porous in the metallic foam and high compaction speed ($S = 10$ mm/min) which is useful because it reduces the process time, while $C_{\%}$ should be the lowest (i.e. $C_{\%} = 40\%$) in order to achieve high energy absorption in combination with small deformation.

Finally, comparing the experimental results (red dots, Figs. 7, 8, and 9) with the fuzzy-GA maps, it is possible to confirm the validity of the proposed model. In fact, the red dots appear to be present only in the shaded areas and in particular in the darkest ones. This suggests the ability of such a model to simulate the strong inherent variability of the aluminum foam manufacturing process and to predict the best combination of the input parameter in order to satisfy the fixed outputs, which in this case are the energy absorption and the compressive deformation.

4 Conclusions

This work deals with the proposal of a combined fuzzy-genetic algorithm methodology able to model the experimental data available from a metal foam manufacturing process. The aim of such a method is to select the manufacturing operational parameters in order to obtain the desired process output, i.e., the absorption energy and the deformation during a compressive test, and, as additional information, understand how much the uncertainty of the model and the process varies by changing those operational parameters.

The input parameters were considered as triangular fuzzy numbers, and the Transformation Method was used to handle uncertainty propagation to the response variables. The genetic algorithm is used to optimize the support of each fuzzy parameter in order to find the best combination in terms of the maximum number of experimental data considered and the hypervolume containing such data.

The variability of the process is highlighted by the fuzzy model through the bands of uncertainty that occur in all the process maps generated. It is important to notice that this information is not available by considering just the nominal regression model, nor directly obtained from the values of the confidence interval.

For the purpose of energy absorption during the crash of vehicles, it is necessary to maximize the energy absorbed during the impact while reducing the maximum deformation in order to maintain the adequate space in passenger cell. Therefore, the fuzzy model was inverted in order to assess the optimal parameters needed for this aim: by using the largest mesh size of carbamide particles and the highest compaction speed, the best results in terms of energy absorption, deformation, and uncertainty level can be achieved while using 40% of carbamide, while for 50% of carbamide particles, only a lower level of absorbed energy is achievable, i.e., the maximum absorption energy is about 55% of the highest value obtained in the experimental tests.

In conclusion, as highlighted by the matching of the experimental results with the darkest areas of the fuzzy maps, which represents the most suitable combination of input parameters for a desired output, the fuzzy-genetic algorithm can be considered a valid and helpful tool in predicting, controlling, and managing the output variables, proving to be practical for modeling complex and variable manufacturing processes.

References

1. Guarino S, Barbieri M, Pasqualino P, Bella G (2017) Fabrication and characterization of an innovative heat exchanger with open cell aluminum foams. Energy Procedia 118:227–232. https://doi.org/10.1016/j.egypro.2017.07.015
2. Banhart J (2000) Manufacturing routes for metallic foams. JOM 52: 22–27. https://doi.org/10.1007/s11837-000-0062-8
3. Ashby MF, Evans AG, Fleck NA, Gibson LJ, Hutchinson JW, Wadley HNG (2000) Metal foams: a design guide
4. Liu J, He S, Zhao H, Li G, Wang M (2018) Experimental investigation on the dynamic behaviour of metal foam: from yield to densification. Int J Impact Eng 114:69–77. https://doi.org/10.1016/j.ijimpeng.2017.12.016
5. Koohbor B, Kidane A (2016) Design optimization of continuously and discretely graded foam materials for efficient energy absorption. Mater Des 102:151–161. https://doi.org/10.1016/j.matdes.2016.04.031
6. Xie B, Fan YZ, Mu TZ, Deng B (2017) Fabrication and energy absorption properties of titanium foam with CaCl 2 as a space holder. Mater Sci Eng A 708:419–423. https://doi.org/10.1016/j.msea.2017.09.123
7. Barbieri M, Di Ilio G, Patanè F, Bella G (2017) Experimental investigation on buoyancy-induced convection in aluminum metal foams. Int J Refrig 76:385–393. https://doi.org/10.1016/j.ijrefrig.2016.12.019
8. Chiappini D (2018) Numerical simulation of natural convection in open-cells metal foams. Int J Heat Mass Transf 117:527–537. https://doi.org/10.1016/j.ijheatmasstransfer.2017.10.022
9. Bai W, Yuan X, Liu X (2017) Numerical investigation on the performances of automotive thermoelectric generator employing metal foam. Appl Therm Eng 124:178–184. https://doi.org/10.1016/j.applthermaleng.2017.05.146
10. Nawaz K, Bock J, Jacobi AM (2017) Thermal-hydraulic performance of metal foam heat exchangers under dry operating conditions. Appl Therm Eng 119:222–232. https://doi.org/10.1016/j.applthermaleng.2017.03.056
11. Orihuela MP, Shikh Anuar F, Ashtiani Abdi I, Odabaee M, Hooman K (2018) Thermohydraulics of a metal foam-filled annulus. Int J Heat Mass Transf 117:95–106. https://doi.org/10.1016/j.ijheatmasstransfer.2017.10.009
12. Guarino S, Di Ilio G, Venettacci S (2017) Influence of thermal contact resistance of aluminum foams in forced convection: experimental analysis. Materials (Basel) 10:907. https://doi.org/10.3390/ma10080907
13. Kremer K (2004) Metal foams for improved crash energy absorption in passenger equipment. http://onlinepubs.trb.org/onlinepubs/archive/studies/idea/finalreports/highspeedrail/hsr-34final_report.pdf (accessed February 5, 2018).
14. Barletta M, Gisario A, Guarino S, Rubino G (2009) Production of open cell aluminum foams by using the dissolution and sintering process (DSP). J Manuf Sci Eng 131:041009. https://doi.org/10.1115/1.3159044
15. Costanza G, Dodbiba G, Tata ME (2016) Optimization of the process parameters for the manufacturing of open-cells iron foams with high energy absorption. Procedia Struct Integr 2:2277–2282. https://doi.org/10.1016/j.prostr.2016.06.285
16. Lázaro J, Solórzano E, Rodríguez-Pérez MA (2014) Alternative carbonates to produce aluminium foams via melt route. Procedia Mater Sci 4:275–280. https://doi.org/10.1016/j.mspro.2014.07.557
17. Lázaro J, Solórzano E, Rodríguez-Pérez MA, Rämer O, García-Moreno F, Banhart J (2014) Heat treatment of Aluminium foam precursors: effects on foam expansion and final cellular structure. Procedia Mater Sci 4:287–292. https://doi.org/10.1016/j.mspro.2014.07.559.
18. A. Byakova, Y. Bezim'yanny, S. Gnyloskurenko, T. Nakamura, Fabrication method for closed-cell aluminium foam with improved sound absorption ability, Procedia Mater Sci 4 (2014) 9–14. doi: https://doi.org/10.1016/j.mspro.2014.07.573.
19. Bai M, Chung JN (2011) Analytical and numerical prediction of heat transfer and pressure drop in open-cell metal foams. Int J Therm Sci 50:869–880. https://doi.org/10.1016/j.ijthermalsci.2011.01.007
20. Woudberg S, Du Plessis JP (2016) An analytical Ergun-type equation for porous foams. Chem Eng Sci 148:44–54. https://doi.org/10.1016/j.ces.2016.03.013
21. Stark JR, Prasad R, Bergman TL (2017) Experimentally validated analytical expressions for the thermal efficiencies and thermal resistances of porous metal foam-fins. Int J Heat Mass Transf 111: 1286–1295. https://doi.org/10.1016/j.ijheatmasstransfer.2017.03.041
22. Wang Y, Zhai X, Wang W (2017) Numerical studies of aluminum foam filled energy absorption connectors under quasi-static compression loading. Thin-Walled Struct 116:225–233. https://doi.org/10.1016/j.tws.2017.03.032
23. Rajak DK, Kumaraswamidhas LA, Das S (2017) On the influence of porosity and pore size on AlSi17 alloy foam using artificial neural network. Ciência Tecnol Dos Mater 29:14–21. https://doi.org/10.1016/j.ctmat.2017.05.004
24. Raj RE, Daniel BSS (2008) Prediction of compressive properties of closed-cell aluminum foam using artificial neural network. Comput Mater Sci 43:767–773. https://doi.org/10.1016/j.commatsci.2008.01.041
25. Jamshidi-Alashti R, Mohammadi Zahrani M, Niroumand B (2013) Use of artificial neural networks to predict the properties of replicated open-cell aluminum alloy foam via processing parameters of melt squeezing procedure. Mater Des 51:1035–1044. https://doi.org/10.1016/j.matdes.2013.05.026
26. Karen I, Yazici M, Shukla A (2016) Designing foam filled sandwich panels for blast mitigation using a hybrid evolutionary optimization algorithm. Compos Struct 158:72–82. https://doi.org/10.1016/j.compstruct.2016.07.081
27. Rodger JA (2014) Application of a Fuzzy Feasibility Bayesian Probabilistic Estimation of supply chain backorder aging, unfilled backorders, and customer wait time using stochastic simulation with Markov blankets. Expert Syst Appl 41:7005–7022. https://doi.org/10.1016/j.eswa.2014.05.012
28. Pandey AK, Dubey AK (2013) Fuzzy expert system for prediction of kerf qualities in pulsed laser cutting of titanium alloy sheet. Mach Sci Technol 17:545–574. https://doi.org/10.1080/10910344.2013.806182
29. Suarez Andrade HI, Hernández Rojas ME, Palomar Pardavé ME, Pimiento SB, Suarez, -Andrade HI, Hernández, - Rojas ME, Palomar - Pardavé ME, Báez, - Pimiento S (2013) Manufacturing of aluminum foams using the sintering dissolution process. Rev Colomb Mater N 5:292–298 http://aprendeenlinea.udea.edu.co/revistas/index.php/materiales/article/viewFile/19235/16521 (accessed January 9, 2018)
30. Ponticelli GS, Guarino S, Giannini O (2017) A fuzzy logic-based model in laser-assisted bending springback control. Int J Adv Manuf Technol 95(1–12):3887–3898. https://doi.org/10.1007/s00170-017-1482-8
31. Aravind S, Shunmugesh K, Biju J, Vijayan JK (2017) Optimization of micro-drilling parameters by Taguchi grey relational analysis. Mater Today Proc 4:4188–4195. https://doi.org/10.1016/j.matpr.2017.02.121
32. Cortés Sáenz D, Gordillo Castillo N, Riba Romeva C, Lloveras Macià J (2015) A fuzzy approach for the selection of non-traditional sheet metal cutting processes. Expert Syst Appl 42: 6147–6154. https://doi.org/10.1016/j.eswa.2015.03.030

33. Susilawati A, Tan J, Bell D, Sarwar M (2015) Fuzzy logic based method to measure degree of lean activity in manufacturing industry. J Manuf Syst 34:1–11. https://doi.org/10.1016/j.jmsy.2014.09.007
34. Taheri SM (2003) Trends in fuzzy statistics. AUSTRIAN J Stat 32: 239–257 http://www.statistik.tuwien.ac.at/oezstat/ausg033/papers/taheri.pdf (accessed July 4, 2017)
35. Haag T, Herrmann J, Hanss M (2010) Identification procedure for epistemic uncertainties using inverse fuzzy arithmetic. Mech Syst Signal Process 24:2021–2034. https://doi.org/10.1016/j.ymssp.2010.05.010
36. Hanss M (2002) The transformation method for the simulation and analysis of systems with uncertain parameters. Fuzzy Sets Syst 130: 277–289 www.elsevier.com/locate/fss (accessed July 5, 2017)
37. Moore MJ, R E, Kearfott R B (1966) Cloud, introduction to interval analysis
38. Dao SD, Abhary K, Marian R (2017) A bibliometric analysis of genetic algorithms throughout the history. Comput Ind Eng 110: 395–403. https://doi.org/10.1016/j.cie.2017.06.009
39. Esen İ, Koç MA (2015) Optimization of a passive vibration absorber for a barrel using the genetic algorithm. Expert Syst Appl 42: 894–905. https://doi.org/10.1016/j.eswa.2014.08.038
40. Goodall R, Marmottant A, Salvo L, Mortensen A (2007) Spherical pore replicated microcellular aluminium: processing and influence on properties. Mater Sci Eng A 465:124–135. https://doi.org/10.1016/j.msea.2007.02.002
41. Montgomery DC (2009) Introduction to statistical quality control, sixth edit. Wiley http://dl4a.org/uploads/pdf/581SPC.pdf (accessed October 2, 2018)